in ENDOR spectra when H_0 is set to position A of the EPR spectrum. In fact, sample calculations based on the atomic coordinates derived from modeling studies show that the largest deviation of r from the molecular plane of the spin-label is ~21° and corresponds to the electron-fluorine separation of 7.2 Å of the ortho-fluorinated derivative (cf. Table III). This comparison provides support for the adequacy of the model chosen for spectral simulations in this study. A more quantitative estimate of this angle, however, depends either on the detection of some feature for which the ENDOR shift depends on H_0 or on simulation of the ENDOR spectra with a more detailed approach to modeling of the intensities of the first derivative features and the single-crystal EPR line widths, perhaps by incorporating the anisotropy of relaxation effects.[55]

The parallel and perpendicular features in the fluorine ENDOR spectra of IV exhibit line widths of approximately 20 kHz. Line widths of other features were also approximately 20 kHz although overlap of features made their measurement difficult. The line width of the ENDOR resonance feature limits the accuracy for separating classes of nuclei on the basis of r. For a peak-to-peak separation of 20 kHz for the detectable ENDOR absorptions, we may expect to resolve the resonance features of classes of protons for which the electron-nucleus separation differs by about 0.2 Å for r values of about 7 Å. For separations of ~10 Å, the values of r must differ by ~1 Å for 20-kHz line widths. This level of resolution is confirmed experimentally at the 7-Å range by the observation of distinguishable features from the two ortho protons in III and IV and at the 10-Å range by the distinguishable features from the meta and para protons of III and the meta protons of IV. Because of the similar g_n values of proton and fluorine nuclei, these estimates are approximately correct for fluorine as well.

The accuracy of measurements of r from hfc constants can be assessed on the basis of the molecular models. As the assignment of the coordinates of the electronic point-dipole of the nitroxyl group was changed from $\rho_N = 0.8/\rho_O = 0.2$ to $\rho_N = 0.5/\rho_O = 0.5$, the values of r calculated from hfc constants and from models disagreed by less than 5%. For instance, for fluorine the average deviation and root-mean-square of the deviation of r were -0.29 and 0.33 Å for $\rho_N = 0.8$ and 0.06 Å and 0.18 Å for $\rho_N = 0.5$, respectively. The assignment of $\rho_N = 0.5/\rho_O = 0.5$, in general, yielded the best agreement between the ENDOR determined values of r and those calculated from molecular models.

It is, thus, evident that ENDOR spectroscopy of spin-labeled compounds provides a generally applicable method of noncrystallographic structure determination of molecules in frozen solutions or polycrystalline systems through measurements of electron-nucleus distances in the range from 5 to 11 Å for protons and fluorines. In addition to their extensive use in EPR spectroscopy,[9-12] spin-labels may find another role in magnetic resonance as probes of molecular geometry through ENDOR spectroscopy to provide an accurate noncrystallographic method for structure determination of immobilized molecules in solution.

(55) (a) Narayama, P. A., Bowman, M. K.; Becher, D.; Devan, L. *J. Chem. Phys.* **1977**, *67*, 1990-1996. (b) Kevan L. Narayana, P. A.; Toriyama, K.; Iwasaki, M. *J. Chem. Phys.* **1979**, *70*, 5006-5014.

Nuclear Magnetic Resonance Study of the Molecular and Electronic Structure of the Stable Green Sulfhemin Prosthetic Group Extracted from Sulfmyoglobin

Mariann J. Chatfield, Gerd N. La Mar,* W. O. Parker, Jr., Kevin M. Smith, Hiu-Kwong Leung, and Ian K. Morris

Contribution from the Department of Chemistry, University of California, Davis, California 95616. *Received January 25, 1988*

Abstract: The ^1H NMR spectral characteristics of the stable green heme extract sulfhemin C from the terminal alkaline equilibration product of sulfmyoglobin have been investigated in order to completely define its molecular structure and to shed light on the nature of metal-prosthetic group π-bonding as reflected in the contact shift pattern in paramagnetic ferric complexes. A complete stereospecific assignment of the ^1H NMR spectrum of the low-spin dicyano complex was effected by a combination of isotope labeling, spin decoupling, analysis of differential paramagnetic dipolar relaxation, and nuclear Overhauser effect, which confirmed that all functional groups of the precursor hemin are retained with the exception of the saturation of pyrrole B to form a cyclic thiolene. The assignments depended upon the use of a viscous solvent to render NOEs detectable, but it is shown that the combination of NOEs and metal-centered relaxation is sufficient to yield assignment without recourse to isotope labeling, opening the possibility for assignment of the spectra of natural low-spin ferric chlorin complexes. The dicyanosulfhemin C contact shift pattern is shown to reflect primarily π-bonding with the highest filled π MO of the chlorin, as found previously for hemin, except that its metal spin is symmetry-restricted to interacting solely with the pyrroles cis to the saturated ring. The raising of the iron d orbital degeneracy by the ring B saturation provides the explanation of why low-spin ferric sulfhemin C, in contrast to hemin, experiences a negligible perturbation of the contact shift pattern upon incorporation into a protein and why the contact shift pattern does not uniquely identify the saturated pyrrole in a chlorin. The assignment by isotope labeling of the peripheral methyl signals of the high-spin ferric bis(dimethyl sulfoxide) complex of sulfhemin C confirms an electronic structure very similar to that observed upon incorporation into a protein matrix. We also confirm that the unique and sharply attenuated 3-methyl contact shift identifies the saturated ring as pyrrole B and that the assignment of high-spin ferric chlorin peripheral methyl signals will yield the identity of the saturated pyrrole(s).

Sulfhemoglobin is a green pigmented nonfunctional form of hemoglobin that can occur under physiological conditions.[1] Sulfmyoglobin, SMb, is an analogous substance, formed in the laboratory by the sequential reaction of myoglobin with H_2O_2 and thiol, which has been frequently used to facilitate the study of the structural modification of sulfhemoglobin.[2-6] Early work on SMb revealed that a sulfur atom is incorporated into the hemin

(1) Park, C. M.; Nagel, R. L. *N. Engl. J. Med.* **1984**, *310*, 1579-1584.

(2) Berzofsky, J. A.; Peisach, J.; Blumberg, W. E. *J. Biol. Chem.* **1971**, *246*, 3367-3377.

(3) Berzofsky, J. A.; Peisach, J.; Blumberg, W. E. *J. Biol. Chem.* **1971**, *246*, 7366-7372.

0002-7863/88/1510-6352$01.50/0

skeleton, **1**, upon sulfglobin formation, with concomitant saturation

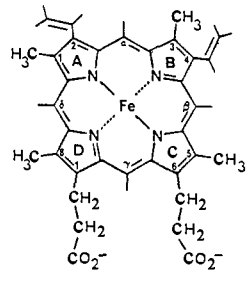

1

of a pyrrole to yield a chlorin-like prosthetic group.[2,6] Detailed NMR studies of sulfmyoglobin have revealed, however, that the protein formed is not homogeneous but can consist of at least three dominant forms, depending on solution conditions.[7-9] These species are the initially formed complex, S_AMb, and the terminal acid, S_BMb, or alkaline, S_CMb, equilibration products.[7-9] The last product, S_CMb, has been demonstrated to be reversibly stable to extraction of its prosthetic group, sulfhemin C, and a combination of isotope labeling and multiplet structure analysis of the vinyl groups led to the proposal[10] for a thiolene structure for ring B, as shown in **2**. A similar conclusion was reached for a derivatized extract for the same SMb.[11]

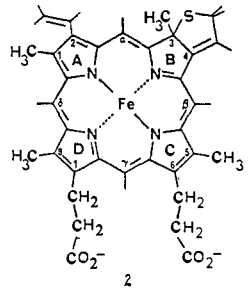

2

Subsequent assignment of the individual heme methyl group signals in all three isomeric SMb's has revealed that their electronic structures are very similar, as reflected in the contact shift patterns, and that the identity of the saturated pyrrole in a sulfhemin, or for that matter in any chlorin, can be uniquely established by NMR in the high-spin but not low-spin ferric derivatives of the corresponding proteins.[12] In order to understand the basis for these structural probes, however, it first becomes necessary to understand the metal–ligand bonding that gives rise to the observed contact shift pattern in a chlorin and then to assess the role of the protein matrix in modulating these interactions. There exists in the literature, however, a paucity of NMR data on iron chlorins,[13-15] and few of the reported spectra have been unambiguously assigned, particularly in the area of natural porphyrin derivatives.[16,17] Such chlorins are of current interest as prosthetic groups in a number of enzyme systems.[18-22] Thus, we pursue a detailed analysis of the sulfhemin C NMR spectrum to completely define its molecular structure as well as elucidate its electronic structure as reflected in the contact shift pattern.[23] These studies will not only shed light directly on the properties of the sulfhemins themselves but may apply to the NMR spectral properties and electron structure of iron chlorins in general.

Table I. Position of the Electronic Absorption Maxima (nm) of the Isomeric Sulfhemin Complexes at 22 °C in 2-Butanone

derivative[a]	sulfhemin A[b]	sulfhemin C[c]	protohemin
Fe^{III}	740	764	640
	606	614	540
	490	486	508
$Fe^{III}(OH^-)$	665	682	606
			576
$Fe^{III}(Im^-)$	592	602	560
			534

[a] Prepared by the method of ref 5. [b] From ref 5; 4 °C. [c] Values vary from those reported previously for an impure sample.[7]

While isotope labeling of the hemin reconstituted into the Mb[24] used to form S_CMb[12] provides some of the required resonance assignments (individual methyls[12] and vinyls[10]), others must be pursued by indirect means, including paramagnetic relaxation[25] and the nuclear Overhauser effect, NOE.[26] The NOE is generally not very useful for paramagnetic complexes, but the use of viscous solvents has been shown to increase cross relaxation so as to allow complete assignments in dicyano hemin.[27] Such a complete assignment for sulfhemin C by indirect NOE and relaxation methods will not only confirm the proposed structure,[10,11] as in **2**, but should establish these methods for providing the needed assignments for other naturally occurring iron–chlorin prosthetic groups[13-22] for which isotope labeling may not be practical. Moreover, the complete assignment of the sulfhemin C NMR spectra will provide both a comparison with the intact protein complex for assigned peaks in the protein,[12] as well as yield the assignment of resonances that are either not resolved or have not been assigned due to the absence of appropriate isotope labels in the protein complex.[12] The characterization of the electronic structure of particularly the low-spin ferric complex is expected to shed light on the reason why the hyperfine shift pattern does not reflect the identity of the saturated pyrrole.[12]

Experimental Section

Sulfhemin C was extracted via the previously described method[10] with samples of metS_CMbCN formed from myoglobin reconstituted with the desired deuterium-labeled hemin.[12] The presence of sulfhemin C was confirmed optically by comparison to the absorption maxima of sulfhemin A and protohemin (Table I). Protohemin reference samples were ob-

(4) Berzofsky, J. A.; Peisach, J. *J. Biol. Chem.* **1972**, *247*, 3774–3782.
(5) Berzofsky, J. A.; Peisach, J.; Horecker, B. L. *J. Biol. Chem.* **1972**, *247*, 3783–3791.
(6) Andersson, L. A.; Loehr, T. M.; Lim, A. R.; Mauk, A. G. *J. Biol. Chem.* **1984**, *259*, 15340–15349.
(7) Chatfield, M. J.; La Mar, G. N.; Balch, A. L.; Lecomte, J. T. J. *Biochem. Biophys. Res. Commun.* **1986**, *135*, 309–315.
(8) Chatfield, M. J.; La Mar, G. N.; Balch, A. L.; Smith, K. M.; Parish, D. W.; LePage, T. J. *FEBS Lett.* **1986**, *206*, 343–346.
(9) Chatfield, M. J.; La Mar, G. N.; Kauten, R. J. *Biochemistry* **1987**, *26*, 6939–6950.
(10) Chatfield, M. J.; La Mar, G. N.; Lecomte, J. T. J.; Balch, A. L.; Smith, K. M.; Langry, K. C. *J. Am. Chem. Soc.* **1986**, *108*, 7108–7110.
(11) Bondoc, L. L.; Chau, M.-H.; Price, M. A.; Timkovich, R. *Biochemistry* **1986**, *25*, 8458–8466.
(12) Chatfield, M. J.; La Mar, G. N.; Smith, K. M.; Leung, H.-K.; Pandey, R. K. *Biochemistry* **1988**, *27*, 1500–1507.
(13) Stolzenberg, A. L.; Strauss, S. H.; Holm, R. H. *J. Am. Chem. Soc.* **1981**, *103*, 4763–4778.
(14) Strauss, S. H.; Silver, M. E.; Long, K. M.; Thompson, R. G.; Hudgens, R. A.; Spartalian, K.; Ibers, J. A. *J. Am. Chem. Soc.* **1985**, *107*, 4207–4215.
(15) Strauss, S. H.; Pawlik, M. J.; Skowyra, J.; Kennedy, J. R.; Anderson, O. P.; Spartalian, K.; Dye, J. L. *Inorg. Chem.* **1987**, *26*, 724–730.
(16) Timkovich, R.; Cork, M. S. *Biochemistry* **1982**, *21*, 5119–5123.
(17) Ikeda-Saito, M.; Inubushi, T. *FEBS Lett.* **1987**, *214*, 111–116.
(18) Morell, D. B.; Chang, Y.; Hendry, I.; Nichol, A. W.; Clezy, P. In *Structure and Function of Cytochromes*; Okunuki, K., Kamen, M., Sekuzu, I., Eds.; University of Tokyo: Tokyo, 1968; pp 563–571.
(19) Lemberg, R.; Barrett, J. In *Cytochromes*; Academic: London, 1973; pp 233–245.
(20) Jacob, G. S.; Orme-Johnson, W. H. *Biochemistry* **1979**, *18*, 2967–2975.
(21) Jacob, G. S.; Orme-Johnson, W. H. *Biochemistry* **1979**, *18*, 2975–2980.
(22) Davis, J. C.; Averill, B. A. *J. Biol. Chem.* **1981**, *256*, 5992–5996.
(23) La Mar, G. N.; Walker (Jensen), F. A. In *The Porphyrins*; Dolphin, D., Ed.; Academic: New York, 1978; Vol. IVB, pp 61–157.
(24) La Mar, G. N.; Toi, H.; Krishnamoorthi, R. *J. Am. Chem. Soc.* **1984**, *106*, 6395–6401.
(25) Swift, T. J. In *NMR of Paramagnetic Molecules*; La Mar, G. N., Horrocks, W. DeW., Jr., Holm, R. H., Eds.; Academic: New York, 1973; pp 53–83.
(26) Noggle, J. H.; Schirmer, R. E. *The Nuclear Overhauser Effect*; Academic: New York, 1971.
(27) Yu, C.; Unger, S. W.; La Mar, G. N. *J. Magn. Reson.* **1986**, *67*, 346–350.

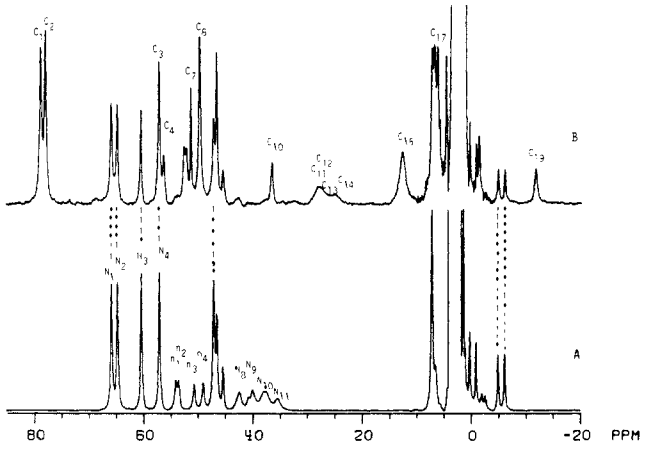

Figure 1. 500-MHz ^{1}H NMR spectra of the high-spin ferric complexes of (A) protohemin IX and (B) 70% sulfhemin C and 30% protohemin IX in DMSO-d_6 at 30 °C. N_i and C_i designate resonances of the $(DMSO)_2$ complexes of protohemin and sulfhemin C, respectively, while n_i designates resonances of the residual five-coordinate chloro complex[31] of protohemin IX.

tained by extraction of the prosthetic group from sperm whale myoglobin under identical conditions. High-spin hemins were prepared by dissolution in DMSO-d_6; low-spin hemins were dissolved in either DMSO-d_6, methanol-d_4, or a solution of 5% methanol-d_4 and 95% ethylene-d_6 glycol, in the presence of excess KCN dissolved in ^2H_2O.

^{1}H NMR spectra were obtained at 30 °C on a Nicolet NT-500 spectrometer operating at 500 MHz. Typical spectra consisted of 5000 transients of 32 768 points over a 100-kHz (high-spin) or 50-kHz (low-spin) bandwidth with a 9-μs 90° pulse. Residual solvent signal was suppressed by a decoupler pulse. All chemical shifts are given in ppm referenced to internal 2,2-dimethyl-2-silapentane-5-sulfonate (DSS) through residual solvent signals. Hemin solutions were 3 mM unless otherwise specified.

^{1}H decoupling, T_1 relaxation, and NOE experiments were observed over a 32-kHz bandwidth with the carrier frequency centered at 24 ppm. Nonselective spin–lattice relaxation measurements were obtained by the standard (180°–τ–90°) inversion-recovery method,[28] with a composite 180° pulse and a repetition rate of 1.2 s^{-1}. T_1 relaxation times were calculated from spectra consisting of 256 scans. NOE spectra were recorded on dicyanosulfhemin C dissolved in methanol-d_4/ethylene-d_6 glycol (see above) by application of a 120-ms presaturation pulse with the decoupler on-resonance; corresponding reference spectra were collected with the decoupler off-resonance. On- and off-resonance spectra were alternated every 64 scans to give a total of 9000 scans with a repetition rate of 0.6 s^{-1}.

Linear combinations of molecular orbitals were obtained by simple Hückel calculations.[29] The labeling of orbital symmetry and energy is that of Gouterman,[30] with symmetry designations numbered from lowest to highest energy orbitals. Asterisks are used to indicate antibonding orbitals.

Results

High-Spin Complexes. The dissolution of native protohemin in DMSO-d_6 yields the spectrum shown in Figure 1A. Peaks N_1–N_4 arise from the ring methyls of the six-coordinate $(DMSO)_2$ complex;[31] the characteristic low-field resonances N_8–N_{11} near 40 ppm arise from the *meso*-H's. A minor contaminant, the five-coordinate chloro–hemin complex, gives rise to methyl peaks n_1–n_4.[31] A DMSO-d_6 solution of sulfhemin C (~70%) and hemin (30%) yields the trace in Figure 1B, for which peaks C_1, C_2, C_8, and C_{17} have three-proton intensity and arise from methyls. The broad single-proton peaks in the range 25–30 ppm must arise from the *meso*-H's of sulfhemin C; no resonances attributable to this complex are detected upfield of −13 ppm.

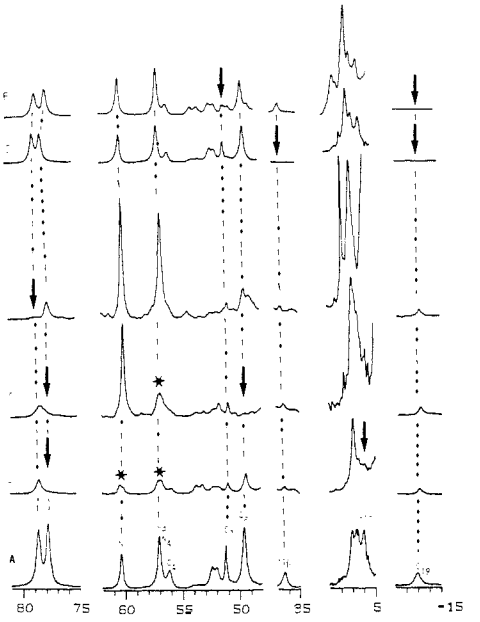

Figure 2. (A) Expanded regions of the 500-MHz ^{1}H NMR spectrum of the high-spin ferric sulfhemin C in DMSO relevant to the assignment of methyl and vinyl resonances. Peaks are labeled as in Figure 1B. Traces B–F provide identical spectral regions of the $(DMSO)_2$ complexes of (B) [1,3-$(C^2H_3)_2$]sulfhemin C, (C) [1,5-$(C^2H_3)_2$]sulfhemin C, (D) [8-(C^2H_3)]sulfhemin C, (E) [2,4-$(^2H_\alpha)_2$]sulfhemin C, and (F) [4-$^2H_3$]-sulfhemin C. Arrows and asterisks mark loss of intensity of resonances due to deuteriation of the sulfhemin C and native protohemin IX complexes, respectively.

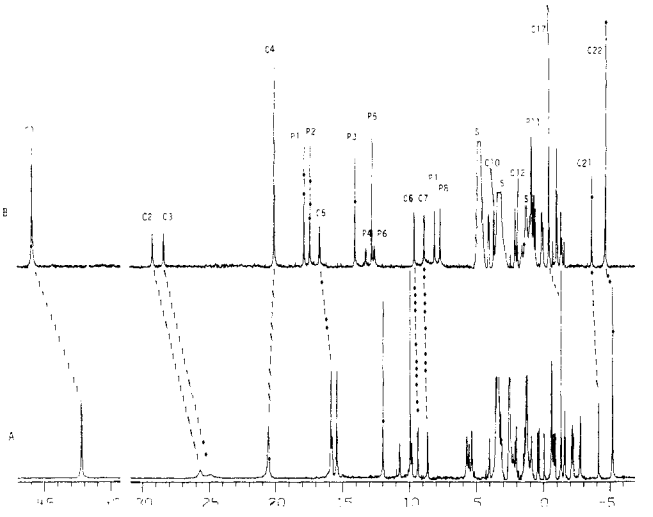

Figure 3. 500-MHz ^{1}H NMR spectra of the low-spin, ferric dicyano complexes of sulfhemin C (3 mM, 30 °C), in (A) DMSO-d_6 and in (B) methanol-d_4. Peaks arising from residual dicyanoprotohemin are labeled as P_i, those of dicyanosulfhemin C, as C_i, and those of solvents, as S; dicyanosulfhemin C peaks whose shifts differ significantly in DMSO and methanol are connected by dotted lines.

Assignment of individual signals of sulfhemin C is illustrated in Figure 2, where trace A displays the regions of the reference spectrum affected by isotope labeling. Deuteriation of methyls 1 and 3 yields the trace in Figure 2B, which identifies unaltered intensity for C_1 and C_8 and reduced intensity for C_2 and C_{17} (expected deuteriation of native hemin is indicated by asterisks),[31] while deuteriation of methyls 1 and 5 (Figure 2C) leaves C_1 unaltered but reduces the intensity of peaks C_2 and C_8; peak C_{17} is obscured by signals from regenerated hemin[10] and other impurities. Deuteriating solely the 8-methyl leads to the trace in Figure 2D that directly confirms C_1 to arise from the 8-CH_3. The remaining methyls are thus C_2 = 1-CH_3, C_8 = 5-CH_3, and C_{17} = 3-CH_3. Deuteriating both the 2- and 4-vinyl group H_α reduces the intensity of single-proton peaks C_{10} and C_{19} (Figure 2E), while

(28) Freeman, R.; Kempsell, S. P.; Levitt, M. H. *J. Magn. Reson.* **1976**, *38*, 453.
(29) Longuet-Higgins, H. C.; Rector, C. W.; Platt, J. R. *J. Chem. Phys.* **1950**, *18*, 1174–1181.
(30) Gouterman, M. In *The Porphyrins*; Dolphin, D., Ed.; Academic: New York, 1978; Vol. IVB, pp 1–165.
(31) Budd, D. L.; La Mar, G. N.; Langry, K. C.; Smith, K. M.; Nayyir-Mazhir, R. *J. Am. Chem. Soc.* **1979**, *101*, 6091–6096.

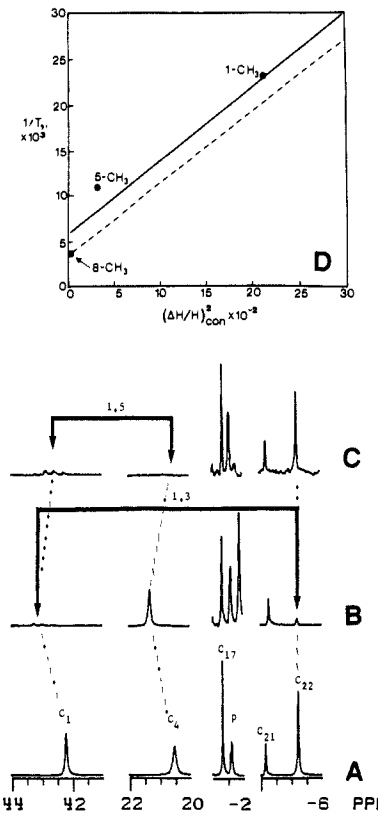

Figure 4. (A) Expanded regions of the 500-MHz ^{1}H NMR spectrum of the dicyano complex of sulfhemin C relevant to the assignment of methyl resonances; peaks are labeled as in Figure 3. Identical regions of the spectra of the dicyano complexes of (B) [1,3-(C^2H_3)$_2$]sulfhemin C and of (C) [1,5-(C^2H_3)$_2$]sulfhemin C provide the methyl assignment, with arrows designating loss of intensity due to deuteriation of sulfhemin C. Peak positions are slightly variable due to aggregation effects.[10] (D) Plot of observed T_1^{-1} versus $[(\Delta H/H)_{con}]^2$ for the methyl groups of the dicyano complexes of sulfhemin C. The solid line is the best fit to the expected[28] straight line. The straight dotted line is that previously obtained for the methyls of a variety of dicyano ferric porphyrins.[32] The intercept at $(\Delta H/H) = 0$ gives the solely metal-centered paramagnetic dipolar contribution to the relaxation rate of heme methyls.[25,32]

deuteriating the 4-vinyl H_α completely and the 4-vinyl H_β partially yields reduced intensity for peaks C_7 and C_{19} (Figure 2F). This uniquely identifies C_{10} as 2-H_α, C_{19} as 4-H_α, and C_7 as one 4-H_β. A possible location for the second 4-H_β is under C_8.

Low-Spin Complexes. Solvent Effects. The original dicyanosulfhemin C spectrum was reported[10] in DMSO-d_6 (Figure 3A; peaks C_i and P_i arise from sulfhemin C and native hemin, respectively), in which isotope labeling and spin decoupling assigned C_5, C_{10}, C_{12} to the intact 2-vinyl H_α, H_β-cis, H_β-trans, and C_6, C_7, C_{21} to the reacted 4-vinyl H_β's and H_α, respectively.[10] The broad peaks near 25 ppm (now labeled C_2 and C_3) were not recognized as sulfhemin C peaks in the earlier spectrum, although it was recognized that the concentration-dependent chemical shifts must reflect aggregation.[10] A superior solvent that yields shifts for the dicyanosulfhemin C complex, which are essentially independent of concentration, is methanol-d_4, with ^{1}H NMR trace shown in Figure 3B. The characteristic multiplets of peaks C_5–C_7, C_{10}, C_{12}, and C_{21} allow the same assignments as in DMSO. More importantly, peaks C_2 C_3, broadened in DMSO, are now sharp in methanol-d_4. A spectrum of dicyanohemin in 95% ethylene-d_6 glycol/5% methanol-d_4 yields a trace (not shown) very similar to, but not quite identical with, that in methanol. The chemical shifts in the three solvents are compared in Table II. Since shifts are invariant upon 3-fold dilution in all but DMSO, the species are assumed to be monomeric, and further experiments are restricted to monomeric species for which the six vinyl protons can be accepted as assigned.

Methyl Assignment. The portions of the ^{1}H NMR trace of dicyanosulfhemin C in DMSO-d_6 where methyl signals resonate

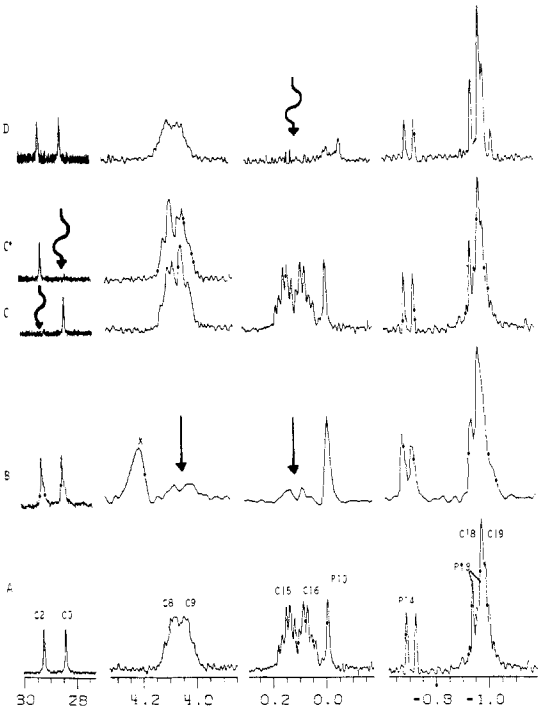

Figure 5. (A) Expanded regions of the 500-MHz ^{1}H NMR reference spectrum of dicyanosulfhemin C in methanol-d_4 at 30 °C relevant to the assignment of the propionate resonances. Peaks from dicyanosulfhemin C are labeled C_i, and those for residual dicyanoprotohemin, P_i. Note that the doublet from the 2-H_β-trans of protohemin (P_{15}) falls on top of the C_{18}, C_{19} multiplet structure. (B) Identical regions for dicyano[6,7-($^2H_\beta$)$_4$]sulfhemin C showing reduced intensities (↓) or C_8, C_9 and C_{15}, C_{16}. (C) Identical regions showing the effect on peak C_8 and C_9 when C_2 is decoupled (↕); decoupling C_3 also influences C_8, C_9 (trace C'). (D) Effect on peaks C_{18} and C_{19} when peaks C_{15} and C_{16} are simultaneously decoupled (↕).

are illustrated in Figure 4A. Traces in parts B and C of Figure 4 are those of the same complex with deuteriation of the 1,3- and 1,5-methyls, respectively, which thus unambiguously identifies C_1 = 1-CH_3, C_4 = 5-CH_3, C_{17} = 8-CH_3, and C_{22} = 3-CH_3. The slight variation in shifts is due to the slight aggregation experienced in this solvent.[10]

Propionate Assignments. Regions of the ^{1}H NMR spectrum of dicyanosulfhemin C in methanol-d_4 where potential propionate signals resonate are illustrated in Figure 5, where all peaks labeled C_i arise from single-proton resonances. Deuteriation of all four propionate H_β's leads to the loss of signals C_8, C_9, C_{15}, and C_{16} and identifies them as the four H_β's (Figure 5B). Irradiation of C_3 or C_2 leads solely to collapse of the multiplet structure of C_8, C_9 (Figure 5C–C'), while similar irradiation of C_{15} and C_{16} (Figure 5D) leads to multiplet collapse of both C_{18} and C_{19}. Thus, C_2, C_3 and C_8, C_9 arise from the α-CH_2 and β-CH_2 of one propionate, and C_{18}, C_{19} and C_{15}, C_{16} arise from the α-CH_2 and β-CH_2 of the other propionate.

***meso*-H Assignment.** A nonselective inversion–recovery experiment was used to determine the T_1 values for all resonances of 3 mM dicyanosulfhemin C in methanol-d_4; the T_1 values are independent of both 3-fold dilution and the presence of ethylene glycol and are listed in Table II. Generally, peaks for the same functional group always relaxed faster in dicyanosulfhemin C than in native dicyanohemin.[32] Since in each complex the four *meso*-H's are by far the closest to the iron and hence relax much faster than any other proton due to the dominance of metal-centered dipolar relaxation,[25,32] the four fastest relaxing protons in a mixture of dicyanosulfhemin C and dicyanohemin must be the four *meso*-H's of the former complex. The partially relaxed spectrum of such a sample 50 ms after inversion (not shown) thus

(32) Unger, S. W.; Jue, T.; La Mar, G. N. *J. Magn. Reson.* **1985**, *61*, 448–456.

Table II. ^{1}H NMR Chemical Shifts of the Dicyano Complex of Sulfhemin C in Various Solvents and Relaxation Data on Dicyanosulfhemin C, Dicyanohemin, and metS$_C$MbCN

		dicyanosulfhemin C						
		obsd shift[a]			hyperfine	$T_1 \times 10^{-1}$,[d]	dicyanohemin:[g]	metS$_C$MbCN:[h]
assignt	peak[b]	*c*	*d*	*e*	shift[f]	ms	$T_1 \times 10^{-1}$, ms	T_1, ms
1-CH_3	C_1	42.19	45.82	46.30	42	4.3	23	19
6-H_α	C_2	25.60	29.20	29.54	25	5.2	19	
6-H_α	C_3	24.80	28.37	28.80	25	5.8	19	
5-CH_3	C_4	20.50	20.07	20.25	16	9.2	19	24
2-H_α	C_5	15.76	16.67	16.31	9	12	35	26
4-H_β	C_6	9.35	9.70	9.89	5	23	33	47
4-H_β'	C_7	8.62	8.80	8.89	5	22	44	41
6-H_β	C_8	5.49	4.08	3.80	0	16	24	
6-H_β'	C_9	3.89	4.04	3.77	0	16	24	
2-H_β-trans	C_{10}	1.97	3.80	3.04	−3	4.7	34	
γ-*meso*-H	C_{11}	3.05	2.09	*i*	−8	4.1	i	
2-H_β-cis	C_{12}	0.29	1.92	1.37	−4	6.4	45	
δ-*meso*-H	C_{13}	*i*	0.71	0.31	−9	3.7	7.3	
α-*meso*-H	C_{14}	*i*	0.59	0.05	−9	2.6	6.8	
7-H_β	C_{15}	−0.80	0.15	−0.12	−4	21	19	
7-H_β'	C_{16}	−0.90	0.08	−0.17	−4	18	19	
8-CH_3	C_{17}	−1.35	−0.40	−0.55	−4	26	18	57
7-H_α	C_{18}	−2.17	−0.95	−1.22	−5	21	24	
7-H_α'	C_{19}	*i*	−0.99	−1.19	−5	21	24	
β-*meso*-H	C_{20}	−2.79	−1.28	−1.99	−11	2.9	7.8	
4-H_α	C_{21}	−4.21	−3.58	−3.80	−11	26	33	32
3-CH_3	C_{22}	−5.24	−4.63	−4.92	−7	9.3	22	29

[a] Shifts in ppm relative to DSS, at 30 °C. [b] Peaks labeled as in Figure 3. [c] 3 mM in DMSO-d_6; shifts are concentration dependent, consistent with aggregation.[10] [d] 3 mM in methanol-d_4, 30 °C, at 500 MHz. [e] Shifts in ppm, in methanol-d_4 at 30 °C, relative to diamagnetic chlorin.[11,37] [f] 3 mM in 95% ethylene-d_6 glycol and 5% methanol-d_4. [g] 3 mM in methanol-d_4, 30 °C, at 500 MHz.[32] [h] 3 mM in ^2H_2O at 30 °C, 500 MHz (assignments from ref 10 and 12). [i] Not detectable.

reveals that only four single-proton signals, C_{11}, C_{13}, C_{14}, and C_{20}, are recovered (and essentially to the same degree), while the remaining signals for dicyanosulfhemin C, and all of the dicyanohemin signals, remain inverted. This clearly identifies collectively the four *meso*-H's of the complex of interest.

The assignment of individual *meso*-H's, as well as those of the individual propionates are effected by NOE measurements.[26] Since NOEs for complexes of this size, particularly when paramagnetic, are generally not detectable in methanol,[27] we turn to a solution of dicyanosulfhemin C in the viscous ethylene-d_6 glycol/methanol-d_4 solution, whose reference trace is illustrated in Figure 6A. Saturation of C_2 (Figure 6B) leads not only to a large (~20%) NOE to C_3, identifying them as geminal partners, but yields a NOE both to C_4, the assigned 5-CH_3, and to C_8, C_9 (propionate H_β's). Thus C_2, C_3 are the 6-propionate α-CH_2 (with C_8, C_9 = β-CH_2), while C_{15}, C_{16}, C_{18}, C_{19} originate from the 7-propionate.

Saturation of the three resolved *meso*-H peaks C_{13} (Figure 6C), C_{14} (Figure 6D), and C_{20} (Figure 6E) yields unique NOEs to C_1 (1-CH_3), C_5 (2-H_α), and C_4 (5-CH_3), respectively, unambiguously establishing the origins as δ-*meso*-H, α-*meso*-H, and β-*meso*-H, in order. The remaining *meso*-H peak, C_{11}, obscured by solvent signals in this solution, must be the γ-*meso*-H. This completes the unique assignment of each proton on dicyanosulfhemin C. The results are summarized in Table II.

Discussion

High-Spin Complexes. The hyperfine shift pattern of sulfhemin C in DMSO-d_6 exhibits downfield contact shifts for pyrrole substituents (except for vinyl H_β's) as well as the apparent *meso*-H's and in that sense is very similar to that exhibited by high-spin ferric porphyrins.[23,31] Moreover, the appearance of downfield, as opposed to upfield, *meso*-H shifts suggests a six-coordinate $(DMSO)_2$ complex, again as observed for hemins.[31] The three intact pyrroles exhibit largely unperturbed contact shifts relative to hemin, with only the methyl (3-CH_3) on the saturated ring (pyrrole B)[10] exhibiting a sharply attenuated contact shift. As proposed earlier,[9,12] this attenuated contact shift for an assigned ring methyl unambiguously identifies the saturated ring.

This pattern of three downfield methyl contact shifts and one (the saturated pyrrole) near 10 ppm is the same as that found in the high-spin ferric complexes of all three isomeric SMb's.[9,12] The $(DMSO)_2$ complexes, however, even for unreacted hemin,

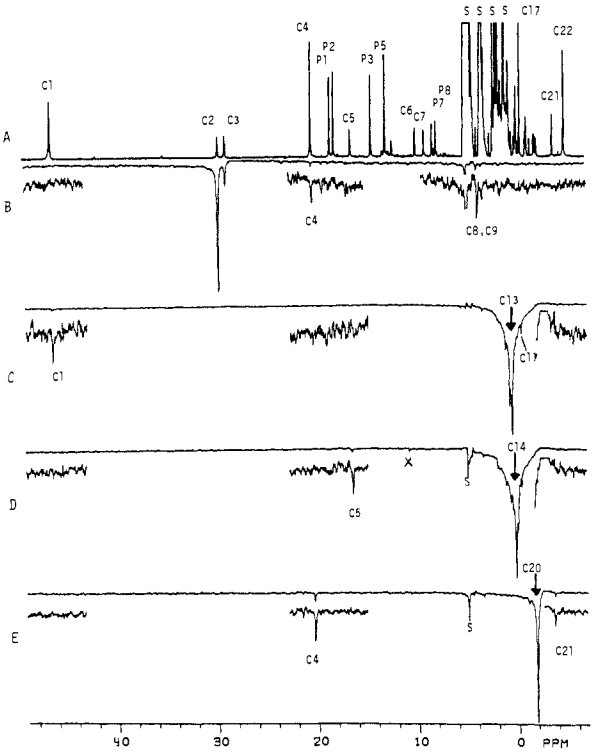

Figure 6. (A) 500-MHz ^{1}H NMR spectrum of 3 mM dicyanosulfhemin C (peaks C_i) in 95% ethylene-d_6 glycol/5% methanol-d_4. Dicyanoprotohemin (peaks P_i) and solvents (peaks S) are also present. NOE difference spectra follow: (B) Irradiation of the more downfield 6-H_α (peak C_2) yields NOEs to the geminal 6-H_α (C_3) and 6-H_β's (C_8,C_9). (C) Irradiation of the *meso*-H peak C_{13} yields an NOE to the 1-CH_3 (peak C_1), identifying it as the δ-*meso*-H; the 8-CH_3 (peak C_{17}) exhibits off-resonance effects. (D) Saturation of the *meso*-H peak C_{14} shows NOE connectivity with the 2-H_α (peak C_5), identifying it as the α-*meso*-H. (E) Saturation of the *meso*-H peak C_{20} produces an intensity change in the 5-CH_3 (peak C_4) and 4-H_α (peak C_{21}), assigning it as the β-*meso*-H.

are not very good models for aquometmyoglobin.[31] Nevertheless, the contact shift patterns for the methyls as well as the downfield *meso*-H contact shifts are essentially the same in the free prosthetic group and in the protein matrix for the sulfhemins. The observed low-field *meso*-H shifts in the high-spin ferric protein complexes of the sulfhemins thus support their designation as aquometmyoglobin complexes with a coordinated water molecule.

The presence of unpaired spin in each of the five iron d orbitals allows for a multiplicity of spin delocalization mechanisms to which both σ- and π-mechanisms contribute.[23,31,33] This multiplicity of mechanisms has precluded detailed analysis of the contact shift pattern even in idealized 4-fold symmetric hemin. Hence, we make no attempt at this time to extend such interpretation to the ferric high-spin sulfhemin C complex. This is better left to the low-spin complexes, which possess a single spin restricted to π-bonding with the macrocycle.[23,34,35]

Low-Spin Complexes. Resonance Assignments. The combination of isotope labeling, differential paramagnetic relaxation effect, and NOEs in viscous solvents provides the complete and unambiguous assignments of both the functional groups and their individual stereospecific protons in dicyanosulfhemin C. All functional groups except those of pyrrole B are intact, as previously proposed.[10] It is noted that while the isotope labeling at the methyls greatly simplified interpretation of the NOE spectra in Figure 6, this isotope labeling was not necessary to effect the assignments in Table II. The identification of the four *meso*-H's by paramagnetic relaxation, the saturation of these four *meso*-H peaks (Figure 6), together with consideration of peak intensity and the additional saturation of the methyl resonances (not shown), would have provided the complete and unique assignments in the absence of the ^2H labeling. Thus, relaxation[32] and NOE in viscous solution[27] provide an important approach that should yield the assignments needed to elucidate the electronic structure in low-spin ferric complexes of other chlorin derivatives.[13-22]

Relaxation Properties. Since both the shifts and T_1's are independent of concentration for dicyanosulfhemin C in methanol-d_4, we conclude that there is negligible aggregation.[36] This is in contrast to DMSO-d_6 solution where both shifts and some line widths are strongly concentration dependent.[10] The failure to identify earlier[10] the peaks C_2, C_3 in DMSO-d_6 must be primarily due to aggregation-caused paramagnetic relaxation, which broadens particularly the 5-CH_3 and 6-propionate peaks (Figure 3). Thus, it appears that the interaction between the sulfhemin C molecules is primarily via propionate groups, as found in other chlorins.[37]

Dipolar relaxation by the unpaired electron dominates proton relaxation in the complexes of interest.[31,32,36] Comparison of the proton T_1 values of dicyanosulfhemin C and native dicyanohemin[32] in Table II reveals that the same functional group generally exhibits shorter T_1's in the former than in the latter species, indicating more efficient electron spin–lattice relaxation in the former. The fact that the four heme methyls exhibit widely different T_1's is due to the relative importance of dipolar relaxation by delocalized spin density versus that by the metal centers, as previously found for dicyanohemins.[32] Since the four *meso*-H shifts exhibit essentially the same T_1 (~30–40 ms), it is likely that they reflect primarily metal-centered relaxation and hence allow comparison to dicyanohemin. The T_1 ratio of dicyanosulfhemin C to dicyanohemin for *meso*-H's (Table II) is ~2. This ratio is confirmed by relaxation of the methyl groups, in that a plot of T_1^{-1}(H) versus the observed contact shift squared for these substituents yields a straight line with intercept for zero contact shift twice that previously reported[28] for dicyanohemin (Figure 4D). Moreover, since the lines for the methyls in sulfhemin C and native hemin are parallel, the relaxation by the delocalized spin most likely originates in the same type of orbital,[23,32] i.e. π MO of the porphyrin or chlorin.

Thus, the T_1(e) (T_1^{-1}(H) $\propto$ T_1(e)) in dicyanosulfhemin C is twice that of dicyanohemin. Moreover, the individual methyls cannot be used as references for determining relative distance from the iron for other protons[38] via the relation $r_i/r_j = (T_1(i)/T_1(j))^{1/6}$ because of the dominance of relaxation by delocalized spin density.[24] The preferred reference signal would therefore be a *meso*-H. This has considerable significance for the ability to assign protons in intact cyanosulfmetmyoglobin complexes using differential relaxation.[38]

Electronic Structure. The NMR spectral characteristics show certain strong similarities between dicyanosulfhemin C and native dicyanohemin[23] (Table II) in that methyl, vinyl H_α, and vinyl H_β's on pyrroles A and C resonate strongly downfield and upfield of their diamagnetic positions, respectively, and the *meso*-H's appear in the window near 0–3 ppm with net upfield hyperfine shifts. On the other hand, the pyrrole D trans to the reacted pyrrole, as well as the reacted pyrrole substituents, exhibits only small and upfield hyperfine shifts. Thus, the spin density in pyrrole A and C exists in a π MO, as found in hemins[23] but with larger magnitude, which is apparently localized on these two pyrroles.

For low-spin hemin, the pattern of large pyrrole C_β and negligible *meso*-C π spin density has shown that π-bonding[23] with the lone spin-containing, essentially degenerate, d_{xz}, d_{yz} occurs predominantly with the $3e_\pi$ (with components $3e_\pi(xz)$ and $3e_\pi(yz)$, as in Figure 7A). The only other MO with symmetry-allowed interaction, $4e_\pi^*$, possesses spin density primarily at the meso positions and hence is not observed to participate.[23] If the degeneracy of the d_{xz}, d_{yz} is raised, the π-spin delocalization is restricted to pyrroles A and C or B and D, depending on whether the lone spin ends up in d_{xz} or d_{yz}, and the contact shifts for the pyrroles A and C or B and D would double, while those for the other two pyrroles would go to zero because the spin occupies either d_{xz} or d_{yz}, not both.[34,35] This general pattern is observed upon imposing the rhombic environment of a protein matrix on low-spin hemin, such as in cyanometmyoglobin, metMbCN.[34,35]

Upon saturating a pyrrole to form a chlorin, the resulting π MOs, which can interact[29] with the iron d_{xz}, d_{yz}, are shown in Figure 7B. The two orbitals, S_6 and A_4, exhibit comparable energies and very similar spin distribution and have metal–ligand π-bonding properties as $3e_\pi(yz)$ and $3e_\pi(xz)$, respectively. Similarly, orbitals comparable to $4e_\pi^*(xz)$ and $4e_\pi^*(yz)$ are S_8^* and A_6^* (Figure 7B). One of the interesting properties of chlorins, as opposed to porphyrins, is that the a_{1u} (A_5 in chlorin) MO is symmetry-forbidden from interacting with d_{xz}, d_{yz} in a porphyrin but is not restricted as such in chlorins.[39,40] The predicted spin distribution for A_5 is included in Figure 7B.

The fact that *meso*-H shifts in dicyanosulfhemin C are small and similar to those in dicyanohemin confirms that iron(III) $\rightarrow$ chlorin π-back-bonding is as weak as in porphyrins;[23] hence, A_6^*, S_8^* do not significantly participate in π-bonding in sulfhemin C. The large π-spin densities exhibited by substituents on pyrroles A and C, and the negligible spin density on *both* pyrroles B and D, are completely consistent with the continued importance of π-bonding with the highest filled π MO known to participate in porphyrins,[34] but with the *lone spin confined solely to* d_{xz} *interacting with* A_4 (Figure 7B). The negligible π-contact shifts for 3-CH_3 can be expected because of the absence of spin density on C_β, whether the spin is in d_{xz} (A_4) or d_{yz} (S_6). However, the absence of π-spin density sensed by 8-CH_3 and 7-α-CH_2 clearly dictates that $S_6(d_{yz})$ does not possess π-spin density. The small net upfield shifts exhibited by 3-CH_3, 8-CH_3, and 7-α-CH_2 are

(33) La Mar, G. N. In *NMR of Paramagnetic Molecules*; La Mar, G. N., Horrocks, W. DeW., Jr.; Holm, R. H., Eds.; Academic: New York, 1973; pp 86–123.
(34) Shulman, R. G.; Glarum, S. H.; Karplus, M. *J. Mol. Biol.* **1971**, *57*, 93–115.
(35) La Mar, G. N. In *Biological Applications of Magnetic Resonance*; Shulman, R. G. Academic: New York, 1979; pp 305–343.
(36) Viscio, D. B.; La Mar, G. N. *J. Am. Chem. Soc.* **1978**, *100*, 8096–8100.
(37) Scheer, H.; Katz, J. J. In *Porphyrins and Metalloporphyrins*; Smith, K. M., Ed.; Elsevier: New York, 1975; pp 399–525.
(38) Cutnell, J. D.; La Mar, G. N.; Kong, S. B. *J. Am. Chem. Soc.* **1981**, *103*, 3567–3572.
(39) Hanson, L. K.; Chang, C. K.; Davis, M. S.; Fajer, J. *J. Am. Chem. Soc.* **1981**, *103*, 663–670.
(40) Chang, C. K.; Hanson, L. K.; Richardson, P. F.; Young, R.; Fajer, J. *Proc. Natl. Acad. Sci. U.S.A.* **1981**, *78*, 2652–2656.

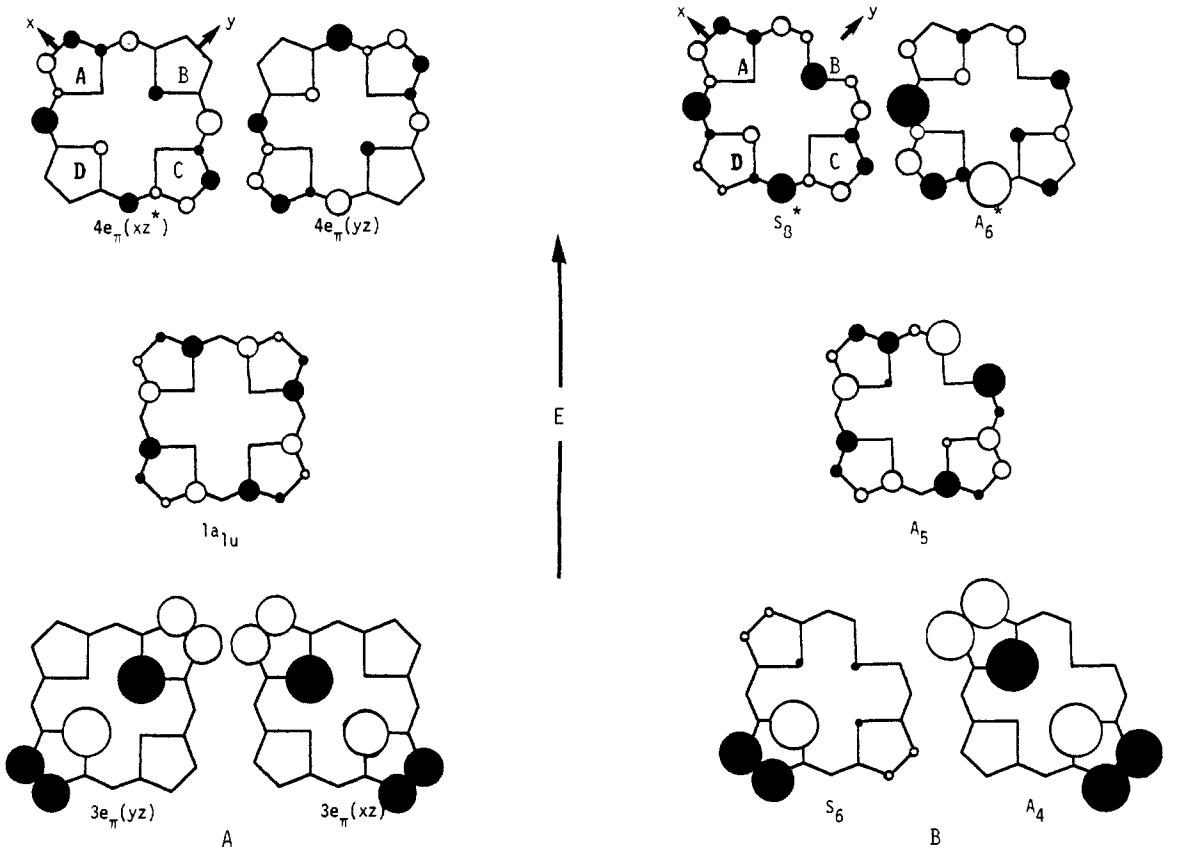

Figure 7. Unpaired spin distribution of molecular orbitals of porphine (A) and chlorin (B), with appropriate symmetry and energy to interact with d_{xz}, d_{yz} iron orbitals.[23,33] Because the A_5 orbital of chlorin can π-bond to the iron,[39,40] the noninteracting porphine counterpart MO, $1a_{1u}$, is shown for comparison. The orientation of axes and labeling of pyrroles are shown at the top of the diagram. Phases are indicated by open and closed circles, with the size of the circle indicating relative spin density. Symmetry and energy designations are those of Gouterman,[30] with increasing number indicating increasing orbital energy and asterisks indicating antibonding orbitals.

consistent with the known axial anisotropy of both low-spin ferric porphyrin[41] and SMb,[2] which have $g_{zz} > g_{xx}, g_{yy}$ and hence yield small (3–5 ppm) upfield dipolar shifts[23,41] for all ring substituents.

The contact shift pattern for both pyrrole substituents as well as *meso*-H's (Table II) is completely consistent with π-bonding between a spin-containing d_{xz} and the A_4 π MO of chlorin. The participation of the A_4 cannot be detected, but it is noted that the spin distribution[39,41] (Figure 7B) places the spin primarily at the saturated pyrrole carbons adjacent to the meso positions, which are not directly sensed by the available substituents.[33] Possible consequences due to spin delocalization into A_5 would be to enhance contact shifts for positions 2 and 5 relative to positions 1 and 6 (Figure 7B). The observed contact shift pattern, however, indicates that the spin density is larger for 1-CH_3 than 2-vinyl and 6-α-CH_2 than 5-CH_3 (Table II).

The chlorin π MO calculations did not include explicitly the proposed[10,11] exocyclic methylene group of sulfhemin C. However, we have shown[12] that the hyperfine shift pattern, and hence unpaired π-spin distribution, is very similar in the three isomeric sulfhemins within the protein matrix, two of which do not possess the added conjugation,[12] indicating that the simple Hückel π MOs provide an adequate qualitative description for sulfhemin C. The details of the role of the exocyclic methylene group are best left to be described by more sophisticated MO calculations.[39,40] Such computations may also shed more light on the characteristic difference of the π-spin density between position 1 and 2 or 5 and 6.

Comparison to Protein Spectra. Inspection of Table II, in which we also include the shifts for the assigned heme substituents of metS_CMbCN,[10,12] reveals that both the shift magnitude and overall pattern for the seven assigned signals (four methyls, three vinyls) are essentially the same in the model complex, dicyanosulfhemin C, and the sulfhemin C incorporated into the protein matrix. Such similarity of shift pattern for a low-spin ferric tetrapyrrole within and outside a protein matrix is unprecedented.[23,33,35,42] The reason for only the small perturbation of the low-spin ferric sulfhemin C shift pattern upon incorporation into the protein is that, unlike a porphyrin, the d_{xz}, d_{yz} degeneracy is not only already resolved in the free sulfhemin C, but the sulfhemin C formation from hemin restricts the lone spin solely to the d_{xz} orbital, as would have resulted upon incorporating an unreacted hemin into the protein.[34,35] Thus, the rhombic perturbation of saturating ring B and the axial perturbation of the histidyl imidazole π-bonding are additive, and hence the protein perturbation, as compared to the bare prosthetic group, is relatively small and comparable for low-spin and high-spin ferric sulfhemin C.

It should be noted that the present description of the π-bonding of chlorins, where the dominant spin-containing orbital encompasses the two unreacted pyrroles cis to the saturated pyrrole (A_4 in Figure 7B), provides the rationale for why the methyl contact shift pattern in low-spin iron(III) chlorin cannot be used to uniquely infer the identity of the saturated ring;[12] only the pair of trans rings can be identified from this pattern, of which one is saturated. The identity of the saturated ring, however, can be unambiguously determined from the contact shift pattern in high-spin ferric chlorins.[12]

Acknowledgment. We are indebted to A. Streitwieser for making available the HMO program and to A. L. Balch, J. Fajer, L. K. Hanson, and S. E. Strauss for helpful discussions. This research was supported by grants from the National Institutes of Health (GM 26226 and HL 22252).

(41) La Mar, G. N.; Walker, F. A. *J. Am. Chem. Soc.* **1973**, *95*, 1782–1790.

(42) Satterlee, J. D. *Annu. Rep. NMR Spectrosc.* **1985**, *17*, 79–178.